Dark vector-gauge-boson model

Subhaditya Bhattacharya, J. Lorenzo Diaz-Cruz, Ernest Ma, and Daniel Wegman

Phys. Rev. D **85**, 055008 — Published 9 March 2012

DOI: 10.1103/PhysRevD.85.055008

UCRHEP-T507

Dark Vector-Gauge-Boson Model

Subhaditya Bhattacharya[1], J. Lorenzo Diaz-Cruz[2], Ernest Ma[1], and Daniel Wegman[1]

[1] *Department of Physics and Astronomy, University of California, Riverside, California 92521, USA*

[2] *Facultad de Ciencias Fisico-Matematicas, Benemerita Universidad Autonoma de Puebla, Puebla, Mexico*

Abstract

A model based on $SU(3)_C \times SU(2)_L \times U(1)_Y \times SU(2)_N$ has recently been proposed, where the $SU(2)_N$ vector gauge bosons are neutral, so that a vector dark-matter candidate is possible and constrained by data to be less than about 1 TeV. We explore further implications of this model, including a detailed study of its Higgs sector. We improve on its dark-matter phenomenology, as well as its discovery reach at the LHC (Large Hadron Collider).

1 Introduction

The nature of dark matter [1] is under intense study. Whereas most assume that it is either a fermion or a scalar or a combination of both [2], the notion that it could be a vector boson just as well has also been proposed. In a theory of universal compact extra dimensions, the first Kaluza-Klein excitation of the standard-model $U(1)$ gauge boson B is such a candidate [3]. The $T-$odd counterpart of B in little Higgs models is another candidate [4]. Non-Abelian vector bosons from a hidden sector may also be considered [5]. All of the above involve "exotic" physics.

Recently, it was realized [6] that an existing conventional model [7] based on superstring-inspired E_6 has exactly the ingredients which allow it to become a model of vector-boson dark matter, where the vector boson itself (X) comes from an $SU(2)_N$ gauge extension of the Standard Model. In this paper we explore further implications of this model, including a detailed study of its Higgs sector and the particle spectrum. We also improve on its dark-matter phenomenology, namely we study the constraints on the parameters of the model from both the relic density as well as the direct dark-matter search. We also study the discovery reach at the LHC (Large Hadron Collider) for the dark vector boson. It should be pointed out that our model is unique. It is the only model of a dark vector boson which is a renormalizable extension of the Standard Model, without a hidden sector. As already mentioned, all other such models involve some kind of "exotic" physics. The fact that our model may have a superstring connection is a bonus, not a requirement.

In Sec. 2 we list all the necessary particles of this (nonsupersymmetric) model. In Sec. 3 we consider the complete Higgs potential and obtain the masses of all the gauge and Higgs bosons. In Sec. 4 we compute the annihilation cross section of the dark-matter vector boson X. In Sec. 5 we study the constraints from dark-matter direct-search experiments. In Sec. 6

we consider some possible signals at the LHC. In Sec. 7 there are some concluding remarks. The details of the Higgs potential are given in the Appendix.

2 Particle content

Under $SU(3)_C \times SU(2)_L \times U(1)_Y \times SU(2)_N \times S$, where $Q = T_{3L} + Y$ is the electric charge and $L = S + T_{3N}$ is the generalized lepton number, the fermions of this nonsupersymmetric model are given by [6]

$$\begin{pmatrix} u \\ d \end{pmatrix} \sim (3, 2, 1/6, 1; 0), \quad u^c \sim (3^*, 1, -2/3, 1; 0), \tag{1}$$

$$(h^c, d^c) \sim (3^*, 1, 1/3, 2; -1/2), \quad h \sim (3, 1, -1/3, 1; 1), \tag{2}$$

$$\begin{pmatrix} N & \nu \\ E & e \end{pmatrix} \sim (1, 2, -1/2, 2; 1/2), \quad \begin{pmatrix} E^c \\ N^c \end{pmatrix} \sim (1, 2, 1/2, 1; 0), \tag{3}$$

$$e^c \sim (1, 1, 1, 1; -1), \quad (\nu^c, n^c) \sim (1, 1, 0, 2; -1/2), \tag{4}$$

where all fields are left-handed. The $SU(2)_L$ doublet assignments are vertical with $T_{3L} = \pm 1/2$ for the upper (lower) entries. The $SU(2)_N$ doublet assignments are horizontal with $T_{3N} = \pm 1/2$ for the right (left) entries. There are three copies of the above to accommodate the known three generations of quarks and leptons, together with their exotic counterparts. It is easy to check that all gauge anomalies are canceled. The extra global U(1) symmetry S is imposed so that $(-1)^L$, where $L = S + T_{3N}$, is conserved, even though $SU(2)_N$ is completely broken. The imposition of S in this case amounts to a generalized lepton number. Such a procedure is very commonplace in model building. For example, to avoid rapid proton decay, an extension of the Standard Model to include supersymmetry requires such an imposition.

The Higgs sector consists of one bidoublet, two doublets, and one triplet:

$$\begin{pmatrix} \phi_1^0 & \phi_3^0 \\ \phi_1^- & \phi_3^- \end{pmatrix} \sim (1, 2, -1/2, 2; 1/2), \quad \begin{pmatrix} \phi_2^+ \\ \phi_2^0 \end{pmatrix} \sim (1, 2, 1/2, 1; 0), \tag{5}$$

$$(\chi_1^0, \chi_2^0) \sim (1, 1, 0, 2; -1/2), \quad \begin{pmatrix} \Delta_2^0/\sqrt{2} & \Delta_3^0 \\ \Delta_1^0 & -\Delta_2^0/\sqrt{2} \end{pmatrix} \sim (1, 1, 0, 3; 1). \tag{6}$$

The allowed Yukawa couplings are thus

$$(d\phi_1^0 - u\phi_1^-)d^c - (d\phi_3^0 - u\phi_3^-)h^c, \quad (u\phi_2^0 - d\phi_2^+)u^c, \quad (h^c\chi_2^0 - d^c\chi_1^0)h, \tag{7}$$

$$(N\phi_3^- - \nu\phi_1^- - E\phi_3^0 + e\phi_1^0)e^c, \quad (E\phi_2^+ - N\phi_2^0)n^c - (e\phi_2^+ - \nu\phi_2^0)\nu^c, \tag{8}$$

$$(EE^c - NN^c)\chi_2^0 - (eE^c - \nu N^c)\chi_1^0, \quad (E^c\phi_1^- - N^c\phi_1^0)n^c - (E^c\phi_2^- - N^c\phi_2^0)\nu^c, \tag{9}$$

$$n^c n^c \Delta_1^0 + (n^c\nu^c + \nu^c n^c)\Delta_2^0/\sqrt{2} - \nu^c\nu^c\Delta_3^0. \tag{10}$$

There are five nonzero vacuum expectation values: $\langle\phi_1^0\rangle = v_1$, $\langle\phi_2^0\rangle = v_2$, $\langle\Delta_1^0\rangle = u_1$, and $\langle\chi_2^0\rangle = u_2$, corresponding to scalar fields with $L = 0$, as well as $\langle\Delta_3^0\rangle = u_3$, which breaks L to $(-1)^L$. Thus m_d, m_e come from v_1, and $m_u, m_{\nu\nu^c}(= -m_{Nn^c})$ come from v_2, whereas $m_h, m_E(= -m_{NN^c})$ come from u_2, and n^c, ν^c obtain Majorana masses from u_1 and u_3. The scalar fields $\phi_3^{0,-}$ and Δ_2^0 have $L = 1$, whereas χ_1^0 has $L = -1$ and Δ_3^0 has $L = 2$.

There are five neutral fermions per family. Two have odd L parity, i.e. ν and ν^c. Their 2×2 mass matrix is of the usual seesaw form, i.e.

$$\mathcal{M}_\nu = \begin{pmatrix} 0 & m_D \\ m_D & M_3 \end{pmatrix}, \tag{11}$$

where m_D comes from v_2 and M_3 from u_3. The other three have even L parity, i.e. N, N^c, and n^c. Their 3×3 mass matrix is given by

$$\mathcal{M}_N = \begin{pmatrix} 0 & -m_E & -m_D \\ -m_E & 0 & m_1 \\ -m_D & m_1 & M_1 \end{pmatrix}, \tag{12}$$

where m_E comes from u_2, M_1 from u_1, and m_1 from v_1. Note that without M_1, the n^c mass would be very small, i.e. $-2m_1 m_D/m_E$. Since $(-1)^L$ is exactly conserved, ν, ν^c do not mix with N, N^c, n^c.

Even though this model is nonsupersymmetric, R parity as defined in the usual way for supersymmetry, i.e. $R \equiv (-)^{3B+L+2j}$, still holds, so that the usual quarks and leptons have even R, whereas $h, h^c, (N, E), (E^c, N^c)$, and n^c have odd R. As for the scalars, (ϕ_1^0, ϕ_1^-), (ϕ_2^+, ϕ_2^0), χ_2^0, Δ_1^0, and Δ_3^0 have even R, whereas (ϕ_3^0, ϕ_3^-), χ_1^0, and Δ_2^0 have odd R.

3 Gauge and Higgs boson masses

The Higgs potential of this model is given by

$$\begin{aligned} V &= \mu_1^2 Tr(\phi_{13}^\dagger \phi_{13}) + \mu_2^2 \phi_2^\dagger \phi_2 + \mu_\chi^2 \chi\chi^\dagger + \mu_\Delta^2 Tr(\Delta^\dagger\Delta) + (\mu_3^2 det\Delta + H.c.) \\ &+ (\mu_{22}\tilde{\chi}\phi_{13}^\dagger\tilde{\phi}_2 + \mu_{12}\chi\Delta\tilde{\chi}^\dagger + \mu_{23}\tilde{\chi}\Delta\chi^\dagger + H.c.) + \frac{1}{2}\lambda_1[Tr(\phi_{13}^\dagger\phi_{13})]^2 + \frac{1}{2}\lambda_2(\phi_2^\dagger\phi_2)^2 \\ &+ \frac{1}{2}\lambda_3 Tr(\phi_{13}^\dagger\phi_{13}\phi_{13}^\dagger\phi_{13}) + \frac{1}{2}\lambda_4(\chi\chi^\dagger)^2 + \frac{1}{2}\lambda_5[Tr(\Delta^\dagger\Delta)]^2 + \frac{1}{4}\lambda_6 Tr(\Delta^\dagger\Delta - \Delta\Delta^\dagger)^2 \\ &+ f_1\chi\phi_{13}^\dagger\phi_{13}\chi^\dagger + f_2\chi\tilde{\phi}_{13}^\dagger\tilde{\phi}_{13}\chi^\dagger + f_3\phi_2^\dagger\phi_{13}\phi_{13}^\dagger\phi_2 + f_4\phi_2^\dagger\tilde{\phi}_{13}\tilde{\phi}_{13}^\dagger\phi_2 + f_5(\phi_2^\dagger\phi_2)(\chi\chi^\dagger) \\ &+ f_6(\chi\chi^\dagger)Tr(\Delta^\dagger\Delta) + f_7\chi(\Delta^\dagger\Delta - \Delta\Delta^\dagger)\chi^\dagger + f_8(\phi_2^\dagger\phi_2)Tr(\Delta^\dagger\Delta) \\ &+ f_9 Tr(\phi_{13}^\dagger\phi_{13})Tr(\Delta^\dagger\Delta) + f_{10}Tr(\phi_{13}(\Delta^\dagger\Delta - \Delta\Delta^\dagger)\phi_{13}^\dagger), \end{aligned} \tag{13}$$

where

$$\tilde{\phi}_2 = \begin{pmatrix} \bar{\phi}_2^0 \\ -\phi_2^- \end{pmatrix}, \quad \tilde{\phi}_{13} = \begin{pmatrix} \phi_3^+ & -\phi_1^+ \\ -\bar{\phi}_3^0 & \bar{\phi}_1^0 \end{pmatrix}, \quad \tilde{\chi} = (\bar{\chi}_2^0, -\bar{\chi}_1^0), \tag{14}$$

and the μ_3^2, μ_{23} terms break L softly to $(-1)^L$.

After the spontaneous breaking of $SU(2)_N \times SU(2)_L \times U(1)_Y$, the gauge bosons $X_{1,2,3}$ and W, Z acquire masses as follows:

$$m_W^2 = \frac{1}{2}g_2^2(v_1^2 + v_2^2), \quad m_{X_{1,2}}^2 = \frac{1}{2}g_N^2[u_2^2 + v_1^2 + 2(u_1 \mp u_3)^2], \tag{15}$$

$$m_{Z,X_3}^2 = \frac{1}{2}\begin{pmatrix} (g_1^2+g_2^2)(v_1^2+v_2^2) & -g_N\sqrt{g_1^2+g_2^2}v_1^2 \\ -g_N\sqrt{g_1^2+g_2^2}v_1^2 & g_N^2[u_2^2+v_1^2+4(u_1^2+u_3^2)] \end{pmatrix}. \tag{16}$$

Whereas the usual gauge bosons have even R, two of the $SU(2)_N$ gauge bosons $X_{1,2}$ have odd R and $X_3(= Z')$ has even R. Assuming that X_1 is lighter than X_2, the former becomes a good candidate for dark matter. There is also $Z - Z'$ mixing in this model, given by $-(\sqrt{g_1^2+g_2^2}/g_N)[v_1^2/(u_2^2+4u_1^2+4u_3^2)]$. This is constrained by precision electroweak data to be less than a few times 10^{-4}. If $m_{Z'} \sim 1$ TeV, then v_1 should be less than about 10 GeV. Now m_b comes from v_1, so this model implies that $\tan\beta = v_2/v_1$ is large and the Yukawa coupling of $bb^c\phi_1^0$ is enhanced. This will have interesting phenomenological consequences [8].

Consider the simplifying (but arbitrary) case of $f_7 = f_{10} = 0$, $\mu_3^2 = 0$, and $\mu_{12} = \mu_{23}$, then from Eqs. (33) and (34) of the Appendix, we find $u_1 = u_3$. The massless states of Eqs. (38) and (39) are then easily identified: $u_2\chi_{1I} + v_1\phi_{3I}$ and $u_2\chi_{1R} + 2\sqrt{2}u_1\Delta_{2R} - v_1\phi_{3R}$ for the longitudinal components of X_1 and X_2 respectively. Three exact mass eigenstates are:

$$(\Delta_{1I} + \Delta_{3I})/\sqrt{2}: \qquad m^2 = -\mu_{12}u_2^2/u_1, \tag{17}$$

$$\Delta_{2I},\ (\Delta_{1R} - \Delta_{3R})/\sqrt{2}: \qquad m^2 = 4\lambda_6 u_1^2 - \mu_{12}u_2^2/u_1. \tag{18}$$

Using the approximation $v_{1,2} << u_{1,2}$, we also have

$$\phi_{3R},\ \phi_{3I}: \qquad m^2 = (f_1 - f_2)u_2^2 - \mu_{22}u_2v_2/v_1, \tag{19}$$

$$(v_2\phi_{1I} + v_1\phi_{2I})/\sqrt{v_1^2 + v_2^2}: \qquad m^2 = -\mu_{22}u_2(v_1^2 + v_2^2)/v_1v_2, \tag{20}$$

$$(2\sqrt{2}u_1\chi_{1R} - u_2\Delta_{2R})/\sqrt{8u_1^2 + u_2^2}: \qquad m^2 = -\mu_{12}(8u_1 + u_2^2/u_1), \tag{21}$$

$$(4u_1\chi_{2I} + u_2\Delta_{1I} - u_2\Delta_{3I})/\sqrt{16u_1^2 + 2u_2^2}: \qquad m^2 = -\mu_{12}(8u_1 + u_2^2/u_1). \tag{22}$$

This pattern shows that (ϕ_1^0, ϕ_1^-) and (ϕ_2^+, ϕ_2^0) behave as the conventional two Higgs doublets with the former coupling to d quarks and and the latter to u quarks. The new feature here is that (ϕ_1^0, ϕ_1^-) also interact with the $SU(2)_N$ gauge bosons and this will be important for the discussion of dark-matter and collider phenomenology in the following.

4 X_1X_1 annihilation

We assume that X_1 is the lightest particle having odd R. It is thus stable and a possible candidate for dark matter. In the early Universe, X_1X_1 will annihilate to particles of even R, i.e. $d\bar{d}$ through h exchange, e^-e^+ through E exchange, $\nu\bar{\nu}$ through N exchange, and $\phi_1\bar{\phi}_1$ through ϕ_3 exchange (and direct interaction). There is also the direct-channel process, such as $X_1X_1 \to \phi_{1R} \to d\bar{d}$, which is suppressed by m_d so it is negligible here. However, the corresponding process for dark-matter direct search, i.e. $X_1d \to X_1d$ through ϕ_{1R} exchange,

may be important as discussed in the next section. Note that there is no tree-level contribution from Z' because the only allowed triple-vector-boson coupling is $X_1 X_2 Z'$ and X_2 is too heavy to be involved.

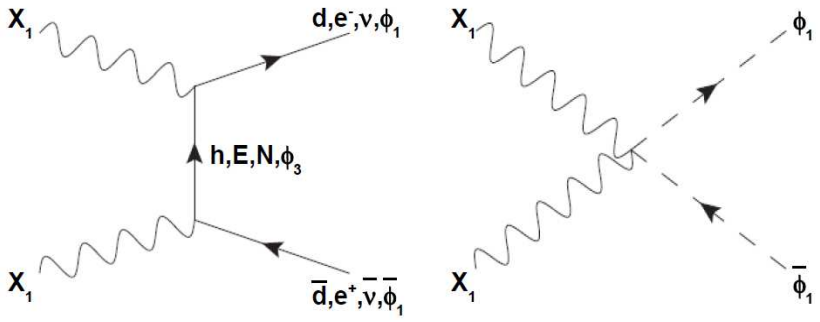

Figure 1: Annihilation of $X_1 X_1$ to standard-model particles.

In Fig. 1 we show the various annihilation diagrams, resulting in the nonrelativistic cross section $\times$ relative velocity given by

$$\begin{aligned} \sigma v_{rel} &= \frac{g_N^4 m_X^2}{72\pi}\left[\sum_h \frac{3}{(m_h^2+m_X^2)^2} + \sum_E \frac{2}{(m_E^2+m_X^2)^2}\right. \\ &+ \left. \frac{2}{(m_{\phi_3}^2+m_X^2)^2} + \frac{1}{m_X^2(m_{\phi_3}^2+m_X^2)} + \frac{3}{8m_X^4}\right], \end{aligned} \tag{23}$$

where the sum over h, E is for 3 families. The factor of 3 for h is the number of colors, and the factor of 2 for E is to include N which has the same mass of E. For the scalar final states $\phi_1 \bar{\phi}_1$, in addition to the exchange of ϕ_3, there is also the direct $X_1 X_1 \phi_1 \bar{\phi}_1$ interaction. Since $v_1 << v_2$, both ϕ_1^0 and ϕ_1^- are physical particles to a very good approximation. Assuming as we do that m_X is the smallest mass in Eq. (23), we must have

$$\sigma v_{rel} < \frac{41 g_N^4}{576\pi m_X^2}. \tag{24}$$

This puts an upper bound on m_X for a given value of σv_{rel}. Assuming $\sigma v_{rel} > 0.86$ pb from

the requirement of relic abundance, and $g_N^2 (\simeq g_2^2) = 0.4$, we then obtain

$$m_X < 1.28 \text{ TeV}. \tag{25}$$

In other words, whereas the scale of $SU(2)_N$ breaking is *a priori* unknown, the assumption of X dark matter constrains it to be of order 1 TeV and be accessible to observation at the LHC.

We consider Eq. (23) as a function of m_X and $\delta = m_h/m_X - 1$, with all three h's having the same mass. We then consider the two extreme cases for the other contributions: one where all heavy masses are equal to m_X; and the other where all heavy masses (except m_X) are equal to the (arbitrary) value $2.5 m_X$ to ensure that no Yukawa or quartic coupling gets too large. In the $\delta - m_X$ plane, for a given value of σv_{rel}, the region between these two lines is then the allowed parameter space for m_X and m_h. We show this in Fig. 2 for $\sigma v_{rel} = 0.91 \pm 0.05$ pb [10].

5 Direct dark matter search

In Fig. 3 we show the tree-level diagrams for $X_1 d \to X_1 d$ through the direct-channel exchange of h and the cross-channel exchange of ϕ_{1R}. Taking into account twist-2 operators and gluonic contributions calculated recently [9] and assuming that $m(h_d) = m(h_s) = m(h_b) = m_h$, we find

$$\begin{aligned} \frac{f_p}{m_p} &= 0.052 \left[-\frac{g_N^2}{4m_\phi^2} - \frac{g_N^2}{16} \frac{m_h^2}{(m_h^2 - m_X^2)^2} \right] + \frac{3}{4}(0.222) \left[-\frac{g_N^2}{4} \frac{m_X^2}{(m_h^2 - m_X^2)^2} \right] \\ &- (0.925) \left((1.19) \frac{g_N^2}{54 m_\phi^2} + \frac{g_N^2}{36} \left[(1.19) \frac{m_h^2}{6(m_h^2 - m_X^2)^2} + \frac{1}{3(m_h^2 - m_X^2)} \right] \right). \end{aligned} \tag{26}$$

To obtain f_n/m_n, the numerical coefficients (0.052,0.222,0.925) in the above are replaced by (0.061,0.330,0.922). The spin-independent elastic cross section for X_1 scattering off a nucleus

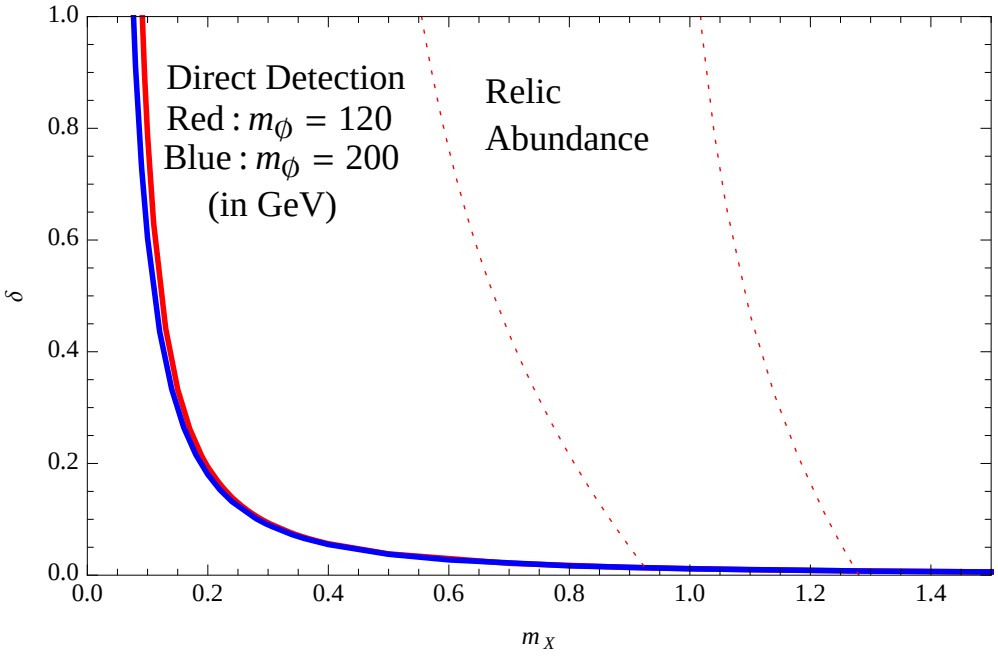

Figure 2: Allowed region in $\delta = m_h/m_X - 1$ versus m_X (in TeV) from relic abundance and from CDMS direct search.

of Z protons and $A - Z$ neutrons normalized to one nucleon is then given by

$$\sigma_0 = \frac{1}{\pi}\left(\frac{m_N}{m_X}\right)^2 \left|\frac{Zf_p + (A-Z)f_n}{A}\right|^2. \tag{27}$$

Here we will use ^{73}Ge with $Z = 32$ and $A - Z = 41$ to compare against the recent CDMS result [11]. In the range $0.3 < m_X < 1.0$ TeV, the experimental upper bound is very well approximated by [12]

$$\sigma_0 < 2.2 \times 10^{-7} \text{ pb } (m_X/1 \text{ TeV})^{0.86}. \tag{28}$$

In Fig. 2 this appears as a solid line for $m_\phi = 120$ GeV, to the right (left) of which is allowed (forbidden) by the CDMS data. If $m_\phi > 120$ GeV, this line will move slightly to the left. It is seen that the relic-abundance constraint is indeed allowed, but direct search is still far away from testing this model.

As for indirect searches from the annihilation of dark matter in space and inside the sun

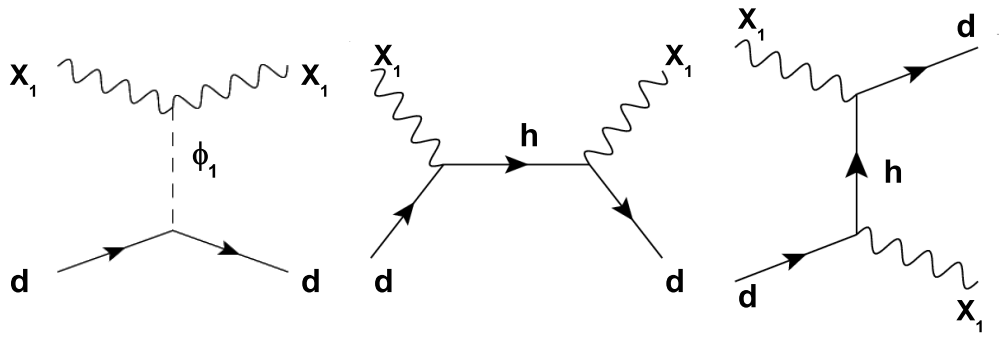

Figure 3: Interactions of X_1 with quarks in direct-search experiments.

or earth, these are subject to more uncertainties (such as contributions from astrophysical sources and the dark-matter density distribution in our galaxy and its capture rates in celestial bodies) beyond what we are able to estimate in this model. In particular, if we regard the satellite observation of a positron excess (with no antiproton excess) as being due to dark-matter annihilation without a boost factor, then this model cannot explain it.

6 Collider phenomenology

The dark-matter gauge boson X_1 may be produced at the Large Hadron Collider in association with the lightest exotic heavy quark h through $d + \text{gluon} \to h + X_1$. Consider the following mass spectrum:

$$m_h > m_{X_2} > m_{E,N} > m_{X_1}. \tag{29}$$

In that case, h may decay into $X_1 d$ and $X_2 d$, then X_2 will decay into $E^+ l^-, E^- l^+, \bar{N}\nu, N\bar{\nu}$, and $E^+ \to X_1 l^+$, $E^- \to X_1 l^-$, $\bar{N} \to X_1 \bar{\nu}$, $N \to X_1 \nu$. This means that about 1/4 of the time, $pp \to hX_1$ will end up with one quark jet + missing energy + $l_i^+ l_j^-$ and $pp \to h\bar{h}$

will end up with two quark jets + missing energy + $l_i^+ l_j^-$. Some of these two-lepton final states could involve different flavors because of mixing of families in the $SU(2)_N$ sector. Note that $X_2 \to X_1 +$ virtual $X_3 \to X_1 + d\bar{d}$ $(l^- l^+)$ is also possible, but very much suppressed if $m_{E,N} < m_{X_2}$. Of course, the hierarchy chosen is not compulsory, other than our stated aim to consider X_1 as a dark vector boson, whereas $m_E = m_N$ is required by the structure of the model. With a different choice of hierarchy, there may not be distinct leptonic final states so the signal will be much more difficult to see. We do not claim that our scenario must be realized, only that it could be realized.

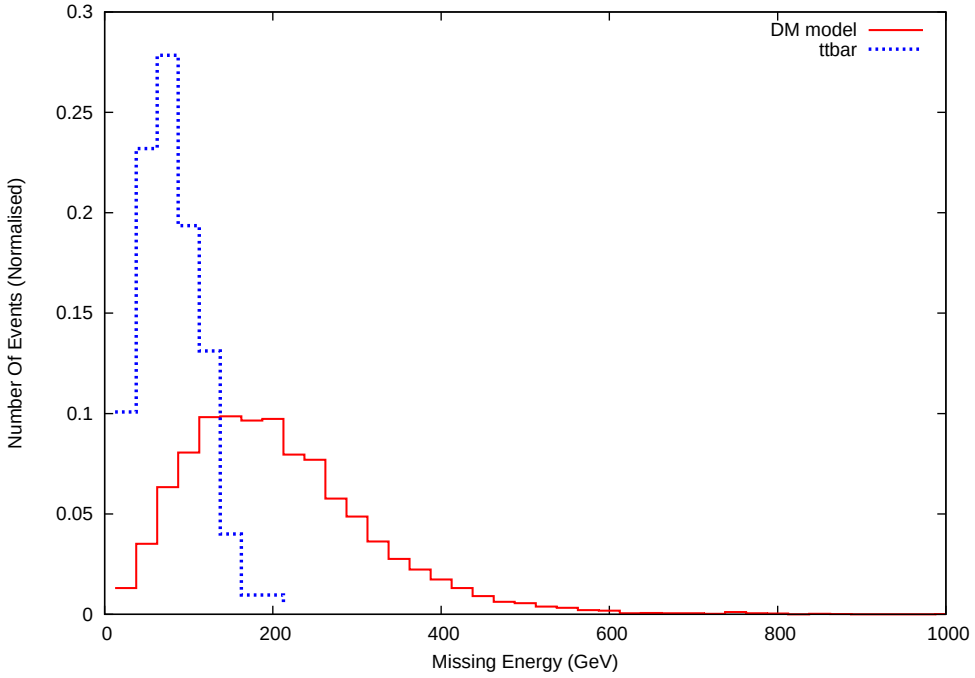

Figure 4: Normalized signal and background distributions as functions of missing transverse energy.

In the following, we choose $m_{X_1} = 700$ GeV, $m_{E,N} = 735$ GeV, $m_{X_2} = 770$ GeV, and $m_h = 980$ GeV. (These values satisfy the constraints from direct detection and relic abundance shown in Fig. 2, and are chosen to optimize the signal. If other points in the allowed region are chosen, the signal to background discrimination would be less, and more integrated

Event rates for $\ell^+\ell^- + 1jet + \not\!\!E_T$ with $p_{T_\ell} > 20$, $p_{T_j} > 50$					
$\not\!\!E_T > 100$		$\not\!\!E_T > 200$		$\not\!\!E_T > 300$	
Signal	Background	Signal	Background	Signal	Background
3.07	237	1.6	0	0.59	0

Table 1: Event rates (fb) for $\ell^+\ell^- + 1$ jet $+ \not\!\!E_T$ at LHC with $E_{cm} = 14$ TeV, using CTEQ6L parton distribution functions, and the average of final-state particle masses as partonic E_{cm}.

luminosity would be required to find the signal.) We find that at the LHC ($E_{cm} = 14$ TeV), the cross section of $dX_1X_1l^-l^+$ production is 5.5 fb. We show in Fig. 4 the distribution of this signal versus the expected standard-model background (dominated by $t\bar{t}$) as a function of missing transverse energy, using the cut $p_T > 20$ GeV for each lepton with $|\eta_l| < 2.5$, and $p_T > 50$ for the one hadronic jet. We use `CalcHEP` [13] in combination with `Pythia` [14] in this calculation. We show in Table 1 that a cut on missing transverse energy of 200 GeV would eliminate the standard-model background which is dominated by $t\bar{t}$ events. We should point out that in this calculation, we have not taken into account a number of experimental issues, such as lepton, jet, or missing-energy smearing, multiple scattering, underlying events, or jet mistag. Uncertainty in jet-energy scale or parton distribution functions may also change the results. We only wish to show that this model has a potentially interesting feature which may help it to be observed at the LHC.

Another possible signal comes from the QCD production of $pp \to h\bar{h}$, with the subsequent decays of h and $\bar{h}$ as discussed before. There are now 2 jets in the final state. In Table 2, we show the opposite-sign dilepton event rates associated with 2 jets and missing energy with the same assumed masses and cuts. We see that whereas the background may be reduced for large missing energy, it is still too big for this search to be successful. The reason is that $t\bar{t}$ production contributes much more two-jet than one-jet events. The production cross section (5.2 fb) for the signal here is about the same as before (5.5 fb) without cuts. (Note that

$pp \to h\bar{h}$ itself is much greater than $pp \to hX_1$ if $m_h = m_X$, but the former is suppressed by phase space because m_h is assumed much greater then m_X, and to reach the dilepton final state, the former is also suppressed by an additional branching fraction.)

Event rates for $\ell^+\ell^- + 2jet + \not{E}_T$ with $p_{T_\ell} > 20$, $p_{T_j} > 50$					
$\not{E}_T > 100$		$\not{E}_T > 200$		$\not{E}_T > 300$	
Signal	Background	Signal	Background	Signal	Background
1.47	348.5	1.04	19.8	0.54	3.96

Table 2: Event rates (fb) for $\ell^+\ell^- + 2$ jets $+ \not{E}_T$ at LHC with $E_{cm} = 14$ TeV, using CTEQ6L parton distribution functions, and the average of final state particle masses as partonic E_{cm}.

If we consider the production of X_1X_1 with a monojet, this suffers from a large $t\bar{t}$ background. With our benchmark point, the signal cross section is 4.2 fb, with a cut of $\not{E}_T >$ 300 GeV, whereas the background is almost 12 fb with the same cuts. This generic process is not helpful for discovering dark matter in our case.

7 Concluding remarks

The (nonsupersymmetric) dark vector-gauge-boson model [6] is studied in some detail. Its complete particle content is delineated and analyzed, including the most general Higgs potential and its minimization. The identification of the X_1 boson as a dark-matter candidate (to account for the observed relic abundance) constrains the $SU(2)_N$ breaking scale to be about 1 TeV. We have updated the theoretical cross section for X_1 to interact in underground direct-search experiments. The present CDMS bound is shown to be much below what is expected in this scenario. On the other hand, the prognosis for observing the consequences of this model at the LHC with $E_{cm} = 14$ TeV and integrated luminosity of 10 fb^{-1} is good, with an expected signal in our specific example of 16 events (dimuon + jet + missing energy) against negligible background for $m_{X_1} = 700$ GeV and $m_h = 980$ GeV.

Appendix

The minimum of V is determined by

$$\begin{aligned} V_0 &= \mu_1^2 v_1^2 + \mu_2^2 v_2^2 + \mu_\chi^2 u_2^2 + \mu_\Delta^2 (u_1^2 + u_3^2) - 2\mu_3^2 u_1 u_3 + 2\mu_{22} v_1 v_2 u_2 + 2\mu_{12} u_1 u_2^2 + 2\mu_{23} u_3 u_2^2 \\ &+ \frac{1}{2}\lambda_1 v_1^4 + \frac{1}{2}\lambda_2 v_2^4 + \frac{1}{2}\lambda_3 v_1^4 + \frac{1}{2}\lambda_4 u_2^4 + \frac{1}{2}\lambda_5 (u_1^2 + u_3^2)^2 + \frac{1}{2}\lambda_6 (u_1^2 - u_3^2)^2 \\ &+ f_2 v_1^2 u_2^2 + f_4 v_1^2 v_2^2 + f_5 v_2^2 u_2^2 + f_6 u_2^2 (u_1^2 + u_3^2) + f_7 u_2^2 (u_3^2 - u_1^2) \\ &+ f_8 v_2^2 (u_1^2 + u_3^2) + f_9 v_1^2 (u_1^2 + u_3^2) + f_{10} v_1^2 (u_1^2 - u_3^2), \end{aligned} \tag{30}$$

where

$$0 = \mu_1^2 + (f_9 + f_{10}) u_1^2 + f_2 u_2^2 + (f_9 - f_{10}) u_3^2 + (\lambda_1 + \lambda_3) v_1^2 + f_4 v_2^2 + \frac{\mu_{22} v_2 u_2}{v_1}, \tag{31}$$

$$0 = \mu_2^2 + f_8 u_1^2 + f_5 u_2^2 + f_8 u_3^2 + f_4 v_1^2 + \lambda_2 v_2^2 + \frac{\mu_{22} v_1 u_2}{v_2}, \tag{32}$$

$$\begin{aligned} 0 &= \mu_\chi^2 + (f_6 - f_7) u_1^2 + \lambda_4 u_2^2 + (f_6 + f_7) u_3^2 + f_2 v_1^2 + f_5 v_2^2 + \frac{\mu_{22} v_1 v_2}{u_2} \\ &+ 2\mu_{12} u_1 + 2\mu_{23} u_3, \end{aligned} \tag{33}$$

$$\begin{aligned} 0 &= \mu_\Delta^2 + (\lambda_5 + \lambda_6) u_1^2 + (f_6 - f_7) u_2^2 + (\lambda_5 - \lambda_6) u_3^2 + (f_9 + f_{10}) v_1^2 + f_8 v_2^2 \\ &+ \frac{\mu_{12} u_2^2}{u_1} - \frac{\mu_3^2 u_3}{u_1}, \end{aligned} \tag{34}$$

$$\begin{aligned} 0 &= \mu_\Delta^2 + (\lambda_5 - \lambda_6) u_1^2 + (f_6 + f_7) u_2^2 + (\lambda_5 + \lambda_6) u_3^2 + (f_9 - f_{10}) v_1^2 + f_8 v_2^2 \\ &+ \frac{\mu_{23} u_2^2}{u_3} - \frac{\mu_3^2 u_1}{u_3}. \end{aligned} \tag{35}$$

There are 22 scalar degrees of freedom, 6 of which become massless Goldstone bosons, leaving 16 physical particles. Their masses are given below:

$$m^2(\phi_3^\pm) = (f_1 - f_2) u_2^2 + 2 f_{10} (u_3^2 - u_1^2) - \lambda_3 v_1^2 + (f_3 - f_4) v_2^2 - \mu_{22} v_2 u_2 / v_1, \tag{36}$$

$$m^2(\sin\beta \phi_1^\pm + \cos\beta \phi_2^\pm) = [f_3 - f_4 - \mu_{22} u_2 / v_1 v_2] \sqrt{v_1^2 + v_2^2}, \tag{37}$$

where $\tan\beta = v_2/v_1$ and the orthogonal combination $\cos\beta \phi_1^\pm - \sin\beta \phi_2^\pm$ is massless, corresponding to the longitudinal component of $W^\pm$. The 5×5 mass-squared matrix spanning

$(\phi_{1I}, \phi_{2I}, \chi_{2I}, \Delta_{1I}, \Delta_{3I})$ is given by

$$\begin{pmatrix} -\mu_{22}v_2u_2/v_1 & -\mu_{22}u_2 & -\mu_{22}v_2 & 0 & 0 \\ -\mu_{22}u_2 & -\mu_{22}v_1u_2/v_2 & -\mu_{22}v_1 & 0 & 0 \\ -\mu_{22}v_2 & -\mu_{22}v_1 & -\frac{\mu_{22}v_1v_2}{u_2} - 4\mu_{12}u_1 - 4\mu_{23}u_3 & -2\mu_{12}u_2 & 2\mu_{23}u_2 \\ 0 & 0 & -2\mu_{12}u_2 & \frac{-\mu_{12}u_2^2+\mu_3^2u_3}{u_1} & \mu_3^2 \\ 0 & 0 & 2\mu_{23}u_2 & \mu_3^2 & \frac{-\mu_{23}u_2^2+\mu_3^2u_1}{u_3} \end{pmatrix}, \tag{38}$$

with two zero mass eigenvalues, spanned by the states $v_1\phi_{1I} - v_2\phi_{2I}$ and $-(v_1/2)\phi_{1I} - (v_2/2)\phi_{2I} + u_2\chi_{2I} - 2u_1\Delta_{1I} + 2u_3\Delta_{3I}$, corresponding to the longitudinal components of Z and Z'. In the $(\chi_{1I}, \Delta_{2I}, \phi_{3I})$ sector, the mass-squared matrix is given by

$$\begin{aligned} & [(f_1 - f_2)v_1^2 + 2f_7(u_1^2 - u_3^2) - \mu_{22}v_1v_2/u_2 - 2(\mu_{12} - \mu_{23})(u_1 - u_3)]\chi_{1I}^2 \\ + \;& 2\sqrt{2}u_2[\mu_{23} - \mu_{12} + f_7(u_1 + u_3)]\chi_{1I}\Delta_{2I} + 2[\mu_{22}v_2 - (f_1 - f_2)v_1u_2]\chi_{1I}\phi_{3I} \\ + \;& [\lambda_6(u_1 + u_3)^2 - \mu_{12}u_2^2/2u_1 - \mu_{23}u_2^2/2u_3 + \mu_3^2(u_1 + u_3)^2/2u_1u_3]\Delta_{2I}^2 \\ - \;& 2\sqrt{2}f_{10}v_1(u_3 + u_1)\Delta_{2I}\phi_{3I} + [(f_1 - f_2)u_2^2 + 2f_{10}(u_3^2 - u_1^2) - \mu_{22}v_2u_2/v_1]\phi_{3I}^2, \end{aligned} \tag{39}$$

with one zero mass eigenvalue, corresponding to the longitudinal component of X_1. The mass-squared matrix of the $(\chi_{1R}, \Delta_{2R}, \phi_{3R})$ sector is analogously given by

$$\begin{aligned} & [(f_1 - f_2)v_1^2 + 2f_7(u_1^2 - u_3^2) - \mu_{22}v_1v_2/u_2 - 2(\mu_{12} + \mu_{23})(u_1 + u_3)]\chi_{1R}^2 \\ + \;& 2\sqrt{2}u_2[\mu_{23} + \mu_{12} + f_7(u_3 - u_1)]\chi_{1R}\Delta_{2R} - 2[\mu_{22}v_2 - (f_1 - f_2)v_1u_2]\chi_{1R}\phi_{3R} \\ + \;& [\lambda_6(u_1 - u_3)^2 - \mu_{12}u_2^2/2u_1 - \mu_{23}u_2^2/2u_3 + \mu_3^2(u_1 - u_3)^2/2u_1u_3]\Delta_{2R}^2 \\ + \;& 2\sqrt{2}f_{10}v_1(u_3 - u_1)\Delta_{2R}\phi_{3R} + [(f_1 - f_2)u_2^2 + 2f_{10}(u_3^2 - u_1^2) - \mu_{22}v_2u_2/v_1]\phi_{3R}^2, \end{aligned} \tag{40}$$

with one zero mass eigenvalue, corresponding to the longitudinal component of X_2. The remaining 5 scalar fields $(\phi_{1R}, \phi_{2R}, \chi_{2R}, \Delta_{1R}, \Delta_{3R})$ form a mass-squared matrix

$$\begin{pmatrix} 2(\lambda_1 + \lambda_3)v_1^2 & 2f_4v_1v_2 & 2f_2v_1u_2 & 2(f_9 + f_{10})v_1u_1 & 2(f_9 + f_{10})v_1u_3 \\ 2f_4v_1v_2 & 2\lambda_2v_2^2 & 2f_5v_2u_2 & 2f_8v_2u_1 & 2f_8v_2u_3 \\ 2f_2v_1u_2 & 2f_5v_2u_2 & 2\lambda_4u_2^2 & 2(f_6 - f_7)u_1u_2 & 2(f_6 + f_7)u_2u_3 \\ 2(f_9 + f_{10})v_1u_1 & 2f_8v_2u_1 & 2(f_6 - f_7)u_1u_2 & 2(\lambda_5 + \lambda_6)u_1^2 & 2(\lambda_5 - \lambda_6)u_1u_3 \\ 2(f_9 - f_{10})v_1u_3 & 2f_8v_2u_3 & 2(f_6 + f_7)u_2u_3 & 2(\lambda_5 - \lambda_6)u_1u_3 & 2(\lambda_5 + \lambda_6)u_3^2 \end{pmatrix}$$

$$+\begin{pmatrix} -\mu_{22}v_2u_2/v_1 & \mu_{22}u_2 & \mu_{22}v_2 & 0 & 0 \\ \mu_{22}u_2 & -\mu_{22}v_1u_2/v_2 & \mu_{22}v_1 & 0 & 0 \\ \mu_{22}v_2 & \mu_{22}v_1 & -\mu_{22}v_1v_2/u_2 & 2\mu_{12}u_2 & 2\mu_{23}u_2 \\ 0 & 0 & 2\mu_{12}u_2 & \frac{-\mu_{12}u_2^2+\mu_3^2u_3}{u_1} & -\mu_3^2 \\ 0 & 0 & 2\mu_{23}u_2 & -\mu_3^2 & \frac{-\mu_{23}u_2^2+\mu_3^2u_3}{u_1} \end{pmatrix}. \quad (41)$$

Acknowledgments

This work is supported in part by the US Department of Energy under Grant No. DE-FG03-94ER40837, and by CONACYT-SNI (Mexico). SB would like to thank Dr. Ehsan Noruzifar for technical help and Dr. AseshKrishna Datta for valuable comments on the numerical simulation.

References

[1] For a review, see for example G. Bertone, D. Hooper, and J. Silk, Phys. Rept. **405**, 279 (2005).

[2] Q.-H. Cao, E. Ma, J. Wudka, and C.-P. Yuan, arXiv:0711.3881 [hep-ph].

[3] G. Servant and T. M. P. Tait, Nucl. Phys. **B650**, 391 (2003).

[4] J. Hubisz and P. Meade, Phys. Rev. **D71**, 035016 (2005).

[5] T. Hambye, JHEP **0901**, 028 (2009).

[6] J. L. Diaz-Cruz and E. Ma, Phys. Lett. **B695**, 264 (2011).

[7] D. London and J. L. Rosner, Phys. Rev. **D34**, 1530 (1986).

[8] C. Balazs, J. L. Diaz-Cruz, H.-J. He, T. M. P. Tait, and C.-P. Yuan, Phys. Rev. **D59**, 055016 (1999).

[9] J. Hisano, K. Ishiwata, N. Nagata, and M. Yamanaka, Prog. Theor. Phys. **126**, 435 (2011).

[10] Particle Data Group: K. Nakamura *et al.*, J. Phys. G: Nucl. Part. Phys. **37**, 075021 (2010).

[11] Z. Ahmed *et al.*, Science **327**, 1619 (2010).

[12] S. Khalil, H.-S. Lee, and E. Ma, Phys. Rev. **D81**, 051702(R) (2010).

[13] A. Pukhov, arXiv:hep-ph/0412191.

[14] T. Sjostrand, S. Mrenna and P. Skands, JHEP **0605**, 026 (2006).